7-2011

Differential Responses of Targeted Lung Redox Enzymes to Rat Exposure to 60 or 85% Oxygen

Zhuohui Gan
Marquette University

David L. Roerig
Medical College of Wisconsin

Anne V. Clough
Marquette University, anne.clough@marquette.edu

Said H. Audi
Marquette University, said.audi@marquette.edu

Differential Responses of Targeted Lung Redox Enzymes to Rat Exposure to 60 Or 85% Oxygen

Zhuohui Gan
Biomedical Engineering, Marquette University, Milwaukee, WI
David L. Roerig
Departments of Anesthesiology and Pharmacology/Toxicology, Medical College of Wisconsin, Zablocki Veterans Affairs Medical Center, Milwaukee, Wi
Anne V. Clough
Departments of Biomedical Engineering, and Mathematics, Statistics and Computer Science, Marquette University, Division of Pulmonary and Critical Care Medicine, Medical College of Wisconsin, Milwaukee, WI
Said H. Audi
Departments of Biomedical Engineering, Marquette University, Division of Pulmonary and Critical Care Medicine, Medical College of Wisconsin, Milwaukee, WI

Journal of Applied Physiology, Vol 111, No. 1 (July 2011): pg. 95-107. DOI.

Abstract: Rat exposure to 60% O_2 (hyper-60) or 85% O_2 (hyper-85) for 7 days confers susceptibility or tolerance, respectively, of the otherwise lethal effects of exposure to 100% O_2. The objective of this study was to determine whether activities of the antioxidant cytosolic enzyme NAD(P)H:quinone oxidoreductase 1 (NQO1) and mitochondrial complex III are differentially altered in hyper-60 and hyper-85 lungs. Duroquinone (DQ), an NQO1 substrate, or its hydroquinone (DQH_2), a complex III substrate, was infused into the arterial inflow of isolated, perfused lungs, and the venous efflux rates of DQH_2 and DQ were measured. Based on inhibitor effects and kinetic modeling, capacities of NQO1-mediated DQ reduction (V_{max1}) and complex III-mediated DQH_2 oxidation (V_{max2}) increased by ~140 and ~180% in hyper-85 lungs, respectively, compared with rates in lungs of rats exposed to room air (normoxic). In hyper-60 lungs, V_{max1} increased by ~80%, with no effect on V_{max2}. Additional studies revealed that mitochondrial complex I activity in hyper-60 and hyper-85 lung tissue homogenates was ~50% lower than in normoxic lung homogenates, whereas mitochondrial complex IV activity was ~90% higher in only hyper-85 lung tissue homogenates. Thus NQO1 activity increased in both hyper-60 and hyper-85 lungs, whereas complex III activity increased in hyper-85 lungs only. This increase, along with the increase in complex IV activity, may counter the effects the depression in complex I activity might have on tissue mitochondrial function and/or reactive oxygen species production and may be important to the tolerance of 100% O_2 observed in hyper-85 rats.

Keywords: oxidative stress, mathematical modeling, duroquinone, cytochrome bc1 complex, cytochrome-*c* oxidase

High o_2 therapy (hyperoxia) is a necessary and effective initial treatment of hypoxemia or low blood Po_2 in adult and pediatric patients with acute lung injury, such as acute respiratory distress syndrome.[50,57] While improving O_2 delivery to vital organs, sustained exposure to O_2 at high fractions (>50%) impairs lung function.[27,38,47] Presently, the underlying mechanisms of lung O_2 toxicity are not fully understood, and new strategies to reduce the toxic effects of this widely used therapy are needed.[4,21]

Several animal models have been developed to evaluate the time course, severity, and pathophysiological mechanisms of lung O_2 toxicity.[24,30,54,69] The rat model is unique in that, when adult rats are exposed to a sublethal 85% O_2 (hyper-85) environment for 5–7 days, they acquire tolerance to the otherwise lethal effects of 100% O_2, in that, if transferred to a 100% O_2 environment, they survive for prolonged periods.[6,24,33] This tolerance is not observed in other rodent species, but a similar tolerance occurs in humans.[19,24,26,32] Conversely, rats exposed to 60% O_2 (hyper-60) for 7 days become more

susceptible to 100% O_2.[23,40] Elucidating the factors that contribute to this tolerance or susceptibility of rats to 100% O_2 will further understanding of the pathogenesis of lung O_2 toxicity. In turn, this may suggest strategies for clinicians at the bedside to protect lung tissue from the toxic effects of sustained exposure to high O_2.[6,24,26,33]

There is ample evidence that the deleterious effects of high O_2 result from increased formation of reactive oxygen species (ROS).[22,31,34,46] Thus previous studies have suggested a role for classic antioxidant enzymes (e.g., superoxide dismutases) in protection from O_2 toxicity.[24,26,42,43] Although the activities of some of these enzymes increase in lung homogenates from rats adapted to lethal hyperoxia, they do not appear to account for all aspects of this adaptive response.[18,23,41,69]

Another proposed mechanism involved in rat tolerance of 100% O_2 is the induction of phase II detoxification enzymes, including NAD(P)H:quinone oxidoreductase 1 (NQO1), glutathione-*S*-transferase, and heme oxygenase-1.[20,48] The induction occurs via the antioxidant response element, in response to oxidative or electrophilic stress.[20,48] Phase II enzymes are, in general, involved in detoxification of reactive electrophilic metabolites via two-electron reduction.[16,20,29] With respect to NQO1, which is predominantly a cytosolic two-electron reductase,[13,55] additional protective effects include regeneration of endogenous and exogenous antioxidants,[12,29,60] scavenging superoxide,[59,71] and competition with prooxidant one-electron quinone reductases (e.g., *P*-450 reductases) for reactive electrophilic metabolites and other redox active compounds.[16,51,55,56,70]

Mitochondrial complexes I and III are a major source of ROS, and their rate of ROS production increases with O_2 tension.[15,66] Thus altering the activity of mitochondrial complex I and/or complex III would be an approach to control the rate of ROS production in response to increased O_2 tension and to protect lung tissue.[18]

To evaluate the activities of redox metabolic processes in a nondestructive manner in isolated perfused lungs, we have pursued the use of indicator dilution methods.[5–7,9,10] These methods involve the bolus injection or finite-pulse infusion of indicators into the lung's arterial inlet, followed by measurement of concentrations of these

Journal of Applied Physiology, Vol 111, No. 1 (July 2011): pg. 95-107. DOI.

indicators in the venous effluent as a function of time. The injected indicators usually include an intravascular indicator plus a test indicator that is a substrate or ligand for the organ's metabolic function(s) of interest. The interactions of the test indicator with metabolic function(s) on passage though the organ result in characteristic differences between the intravascular and test indicator venous effluent concentration vs. time curves. The information in these curves about these metabolic function(s) is then deciphered using mathematical modeling[5,9,10]

Using these indicator dilution methods and mathematical modeling, we have demonstrated that the redox active quinone compound duroquinone (DQ) is reduced to durohydroquinone (DQH_2), and DQH_2 is oxidized to DQ on passage through the pulmonary circulation of the isolated perfused rat lung.[5,6] Based on inhibitor studies, NQO1 was implicated as the dominant DQ reductase and mitochondrial complex III as the dominant DQH_2 oxidase, and the capacities of the lung to reduce DQ to DQH_2 and oxidize DQH_2 to DQ were shown to be measures of lung NQO1 activity and complex III activity, respectively.[5,6]

The objective of the present study was to evaluate the effects of a 7-day exposure of rats to hyper-60 or hyper-85 on activities of NQO1 and complex III in the intact lung using DQ and DQH_2, respectively, as indicator dilution probes. Demonstration that the activity of a particular redox enzyme is differentially altered by exposure to hyper-60 and hyper-85 would suggest a role in the development of the observed rat tolerance of, or susceptibility to, 100% O_2 toxicity.

Methods

Materials.

DQ and other reagent grade chemicals were purchased from Sigma Chemical (St. Louis, MO). Bovine serum albumin (BSA; Standard Powder) was purchased from Serologicals (Gaithersburg, MD). DQH_2 was prepared by reduction of DQ with potassium borohydride, as previously described.[17]

Animals.

For normoxic lung studies, male Sprague-Dawley rats (275–325 g; Charles River) were exposed to room air. For the hyperoxic lung studies, age-matched rats were housed in a Plexiglas chamber maintained at approximately hyper-60 or hyper-85, balance N_2, for 7 days with free access to food and water.[6] The total gas flow was 3.5 l/min, and the chamber CO_2 was maintained at <0.5%. The temperature within the chamber was maintained at 20–22°C. Every other day, the rats were weighed, and their cage, food, water, and CO_2 absorbent were changed. The protocol was approved by the Institutional Animal Care and Use Committees of the Zablocki Veterans Affairs Medical Center and Marquette University (Milwaukee, WI).

Isolated, perfused lung experiments.

As previously described, rats were anesthetized with pentobarbital sodium (40 mg/kg body wt ip), the trachea was clamped, the chest opened, and heparin (0.7 IU/g body wt) injected into the right ventricle. The pulmonary artery and the trachea were cannulated, and the pulmonary venous outflow was accessed via a cannula in the left atrium. The lung was removed from the chest and attached to a ventilation and perfusion system. The control perfusate contained (in mM) 4.7 KCl, 2.51 $CaCl_2$, 1.19 $MgSO_4$, 2.5 KH_2PO_4, 118 NaCl, 25 $NaHCO_3$, 5.5 glucose, and 5% BSA.[5] The single-pass perfusion system was primed (Masterflex roller pump) with the control perfusate maintained at 37°C and equilibrated with 15% O_2, 6% CO_2, balance N_2, resulting in perfusate Po_2, Pco_2, and pH of ~105 Torr, 40 Torr, and 7.4, respectively. Initially, control perfusate was pumped through the lung until it was evenly blanched and venous effluent was clear of blood. The lung was ventilated (40 breaths/min) with end-inspiratory and end-expiratory pressures of ~6 and 3 mmHg, respectively, with the above gas mixture. The pulmonary arterial pressure was referenced to atmospheric pressure at the level of the left atrium and monitored continuously during the course of the experiments. The venous effluent pressure was atmospheric pressure.

Journal of Applied Physiology, Vol 111, No. 1 (July 2011): pg. 95-107. DOI.

Pulse infusion experimental protocols.

To determine the DQ reducing capacity of the lung, four 135-s sequential arterial pulse infusions at DQ concentrations of 50, 100, 200, and 400 μM were carried out with a perfusate flow of 10 ml/min. For each pulse infusion, a venous effluent sample (1 ml) was collected between 130 and 135 s after initiation of the pulse infusion. Infusion for 130 s is long enough for the venous effluent concentrations of DQ and DQH_2 to reach steady state.[5,6] Between pulse infusions, the lung was perfused with 30 ml of fresh perfusate to wash the lung and perfusion system of any remaining traces of DQ and/or DQH_2. For some of the lungs, the 400 μM DQ pulse infusion was repeated after lung treatment with the NQO1 inhibitor dicumarol (400 μM).

To determine the capacity of NQO1-mediated DQ reduction on passage through the pulmonary circulation, each lung was perfused for 5 min with perfusate containing antimycin A (10 μM) to inhibit complex III mediated DQH_2 oxidation.[14] This was followed by four successive DQ pulse infusions, as above, with the inhibitor present throughout the infusion protocol.

To evaluate the capacity of complex III-mediated DQH_2 oxidation on passage through the pulmonary circulation, each lung was perfused for 5 min with perfusate containing dicumarol (NQO1 inhibitor; 400 μM) or dicumarol plus rotenone (complex I inhibitor; 20 μM).[5,6,9] This was followed by four 135-s sequential arterial pulse infusions at DQH_2 concentrations of 50, 100, 200, and 400 μM at a flow of 10 ml/min, with the inhibitors present throughout the infusion protocol. A 1-ml venous effluent sample was collected between 130 and 135 s after initiation of each pulse infusion. For some of the lungs, the 400 μM DQH_2 infusion was repeated after lung perfusion with antimycin A.

For determination of perfused lung surface area, a 150 μM 20-s pulse infusion of the angiotensin converting enzyme (ACE) substrate *N*-[3-(2-furyl) acryloyl]-Phe-Gly-Gly (FAPGG) was carried out at a perfusate flow of 30 ml/min.[6] Two 1-ml venous effluent samples were collected between 15 and 20 s after the start of the FAPGG infusion.[6]

Journal of Applied Physiology, Vol 111, No. 1 (July 2011): pg. 95-107. DOI.

Determination of DQ and DQH_2 concentrations in venous effluent samples.

The concentrations of DQ and DQH_2 in the venous effluent samples were determined as previously described.[5] At steady state, 92 ± 3% (SD) and 95 ± 4% (SD) of the infused DQ and DQH_2, respectively, were recovered in the total venous effluent as DQ + DQH_2, with the loss attributable primarily to binding of both forms to the experimental tubing (data not shown).

Steady-state DQH_2 or DQ efflux rates.

The steady-state efflux rates of DQH_2 or DQ from the lung during DQ or DQH_2 arterial infusion were calculated as the product of the perfusate flow (10 ml/min) and the steady-state venous effluent DQH_2 or DQ concentrations, respectively.

Log mean DQ and DQH_2 concentrations.

DQ vascular concentration during DQ arterial infusion decreases as it passes through the capillary region due to reduction. Thus the effective DQ concentration in the capillary region during DQ arterial infusion is given by its log mean,

$$\text{Log mean DQ conc.} = \frac{[\overline{\text{DQ}}]_{\text{in}} - [\overline{\text{DQ}}]_{\text{out}}}{\ln([\overline{\text{DQ}}]_{\text{in}}/[\overline{\text{DQ}}]_{\text{out}})} \quad (1)$$

where $[\overline{\text{DQ}}]_{\text{in}}$ and $[\overline{\text{DQ}}]_{\text{out}}$ are the arterial infused and venous effluent steady-state DQ concentrations, respectively[5] Similarly, the effective DQH_2 concentration in the capillary region during DQH_2 arterial infusion is given by,

$$\text{Log mean DQH}_2\text{ conc.} = \frac{[\overline{\text{DQH}_2}]_{\text{in}} - [\overline{\text{DQH}_2}]_{\text{out}}}{\ln([\overline{\text{DQH}_2}]_{\text{in}}/[\overline{\text{DQH}_2}]_{\text{out}})} \quad (2)$$

Journal of Applied Physiology, Vol 111, No. 1 (July 2011): pg. 95-107. DOI.

where $[\overline{DQH_2}]_{in}$ and $[\overline{DQH_2}]_{out}$ are the arterial infused and venous effluent steady-state DQH_2 concentrations, respectively.

Determination of perfused capillary surface area.

The linear steady-state rate of ACE-mediated FAPGG hydrolysis is represented as a permeability-surface area product (*PS*, ml/min) defined by *Eq. 3* :[6]

$$PS = -F \ln(1 - E) \tag{3}$$

where E = steady-state extraction ratio = $1 - [FAPGG]_o/[FAPGG]_i$; $[FAPGG]_i$ is the infused arterial FAPGG concentration; $[FAPGG]_o$ is the steady-state venous effluent FAPGG concentration calculated as the average [FAPGG] in the collected venous effluent samples; and F is the perfusate flow.[6] In the present study, the *PS* product is considered to be an index of perfused capillary endothelial surface area.[5,6,9]

Lung homogenate NQO1 activity.

For this assay, the lungs were perfused with perfusate containing 2.5% Ficoll instead of 5% BSA, weighed, and placed in ice-cold buffer (5 ml/g lung tissue, pH 7.4) containing (in mM) 10 *N*-2-hydroxyethylpiperazine-*N'*-2-ethanesulfonic acid (HEPES), 250 sucrose, 3 EDTA, 1 phenylmethylsulfonyl fluoride, and 1% protease inhibitor cocktail (Sigma catalog no. P8340). The lungs were first minced and then homogenized at 4°C using a Polytron tissue homogenizer (Kinematica, Luzern, Switzerland). The lung homogenate was centrifuged (12,100 *g*) at 4°C for 30 min, and the supernatant was collected and kept at 4°C. The supernatant protein concentration and NQO1 activity were measured as previously described.[6]

Complexes I and IV assays.

The lungs were perfused with perfusate containing 2.5% Ficoll instead of 5% BSA, weighed, minced, and homogenized as above with buffer (pH 7.2) containing (in mM) 225 mannitol, 75 sucrose, 5 3-(*N*-morpholino)propanesulfonic acid, 20 ethylene glycol-bis(β-aminoethyl

ether)-*N,N,N′,N′*-tetraacetic acid, 2% fatty-acid free BSA, and 0.02 ml/ml protease inhibitor cocktail set III (Calbiochem, La Jolla, CA), utilizing a Polytron tissue homogenizer. Lung homogenates were centrifuged at 1,500 *g* for 5 min at 4°C, and the resulting supernatants were centrifuged again at 13,000 *g* for 30 min at 4°C to obtain a crude mitochondrial fraction (P2). The P2 fractions were washed twice by resuspension in 8 ml ice-cold homogenization buffer without BSA and then centrifuged (13,000 *g* for 20 min at 4°C). The final P2 fractions were resuspended in 1-ml BSA-free homogenization buffer. Complex I activity was measured using the method of Lenaz et al.,[44] as previously described.[9] Mitochondrial complex IV activity was measured as described by Storrie and Madden[61] using ferrocytochrome *c* as the substrate. The protein concentrations were determined as previously described.[6,9]

Total glutathione content.

For this assay, the lungs were perfused with buffer containing (in mM) 10 HEPES, 5 glucose, and 5% dextran (~67,000 mol wt), pH 7.4. The lungs were then dissected free from connective tissue and weighed. The tissue was then placed into 10 volumes (per lung wet weight) of 4°C sulfosalicylic acid (5%), minced, and homogenized as above. The homogenate was centrifuged (10,000 *g*) at 4°C for 20 min, and the supernatant was used to determine total lung glutathione content, as described by Owens and Belcher[49] and modified by Tietze[65] and Griffith.[39]

Statistical evaluation of data.

Statistical comparisons were carried out using *t*-test or ANOVA followed by Tukey's test, with $P < 0.05$ as the criterion for statistical significance.

Results

Rats lost ~14% of their preexposure body weights (Fig. 1) over the 7-day hyper-85 exposure period, consistent with results from previous studies.[24,52] Most of this weight loss occurred between *days 2* and *6*, during which the rats' water and food intake decreased substantially. On the other hand, rats exposed to hyper-60 gained

Journal of Applied Physiology, Vol 111, No. 1 (July 2011): pg. 95-107. DOI.

body weight steadily over the 7-day exposure period at a rate that is virtually the same as that of age-matched normoxic rats.[23] Subsequent determination of model parameters is unaffected by the body weight loss of hyper-85 rats, since normalization is done with respect to dry lung weight rather than body weight.

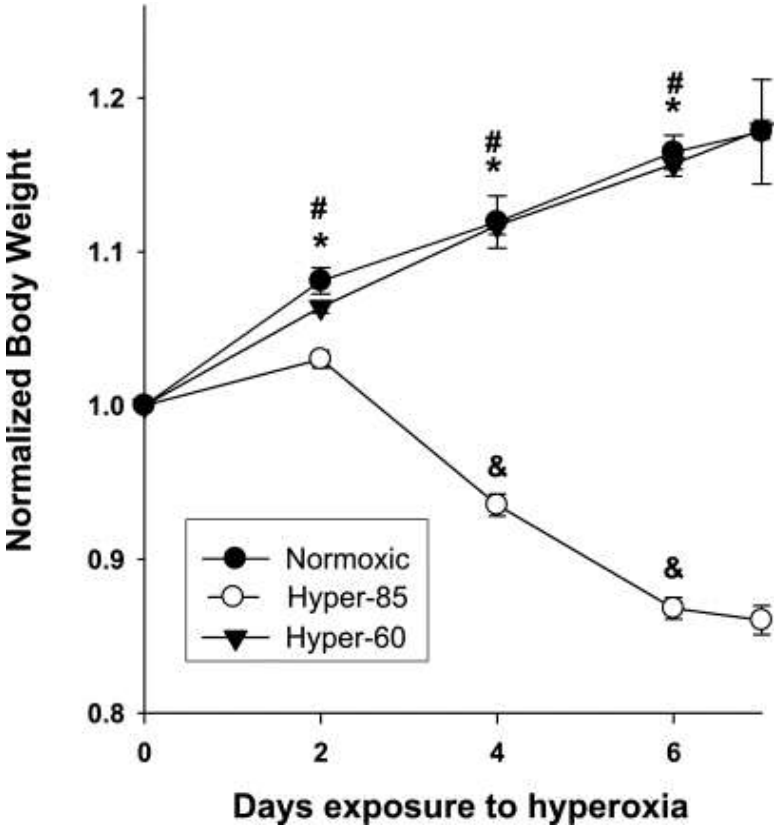

Fig. 1. Rat body weights normalized to preexposure body weights at different time points during the 7-day exposure period to room air (normoxic), 60% O_2 (hyper-60), or 85% O_2 (hyper-85). Values are means ± SE (n = 6, 33, and 34 for normoxic, hyper-60, and hyper-85 rats, respectively). Normalized weights at a given time are significantly different from normalized weights at the previous time point for *normoxic, # hyper-60, or & hyper-85 rats, respectively ($P < 0.05$).

Rat exposure to hyper-85 for 7 days (hyper-85) increased lung wet weight by 87%, with no significant effect on wet-to-dry weight ratio compared with normoxic lungs (Table 1). The lack of a significant difference in wet-to-dry weight ratios between normoxic and hyper-85 lungs (Table 1) is consistent with the finding of Crapo et al.[24] that the increase in wet weight was due to increased tissue mass not edema. Hyper-60 lung wet weights and wet-to-dry weight ratios were not different from normoxic lungs (Table 1).[40]

Journal of Applied Physiology, Vol 111, No. 1 (July 2011): pg. 95-107. DOI.

Table 1. Rat body weights, lung weights, lung wet-to-dry weight ratio, ACE activity, and aortic blood Hct

	Body Weight, g	Wet Weight, g	Wet-to-Dry Ratio	*PS*, ml/min	Hct, %
Normoxic	316 ± 4	1.22 ± 0.03	5.56 ± 0.09	24.7 ± 1.7	43.5 ± 0.4
Hyper-60	302 ± 2*	1.31 ± 0.02	5.45 ± 0.05	25.1 ± 1.4	33.5 ± 0.6*
Hyper-85	311 ± 2	2.29 ± 0.08*†	5.72 ± 0.08	10.7 ± 0.8*†	50.1 ± 0.8*†

Values are means ± SE; *n* values are as follows for body weight, lung wet weight, wet-to-dry ratio, permeability surface area product (*PS*), and hematocrit (Hct), respectively: normoxic lungs, *n* = 38, 38, 31, 19, and 27 (38 is the total number of normoxic rats studied); hyper-60 (60% O_2 exposure) lungs, *n* = 38, 38, 29, 18, and 23 (38 is the total number of hyper-60 rats studied); hyper-85 (85% O_2 exposure) lungs, *n* = 41, 41, 28, 20, and 27 (41 is the total number of hyper-85 rats studied). Body weight is the value at the beginning of the 7-day exposure period. *PS* is measure of angiotensin-converting enzyme (ACE) mediated *N*-[3-(2-furyl) acryloyl]-Phe-Gly-Gly hydrolysis and an index of perfused capillary surface area. Significantly different from * normoxic and †hyper-60 values, $P < 0.05$.

Exposure to hyper-85 for 7 days decreased *PS* (ml/min), an index of perfused capillary endothelial surface area, by 56% compared with normoxic lungs (Table 1). This is consistent with the 50% decrease in capillary volume and endothelial surface area measured morphometrically.[24,25,52] The *PS* values for hyper-60 and normoxic lungs were not significantly different. This is consistent with no change in morphometric measures of capillary volume and endothelial surface area between normoxic and hyper-60 lungs.[40]

Rat exposure to hyper-85 and hyper-60 had a differential effect on aortic blood hematocrit (Table 1). Exposure to hyper-85 increased hematocrit by 16%, while exposure to hyper-60 decreased it by 12% compared with normoxic lungs.[24] The increase in aortic blood hematocrit of hyper-85 rats is consistent with that reported in previous studies.[24,25] Those studies suggested that this decrease could be due to dehydration, consistent with the measured body weight loss in hyper-85 rats (Table 1). There was no significant difference in the isolated lung perfusion pressure at 10 ml/min among the three groups of lungs.[52]

For hyper-60 and hyper-85 lungs, the DQH_2 efflux rates during the arterial infusion of DQ at the two highest concentrations were, on average, 37% higher than in normoxic lungs (Fig. 2). For all three lung groups, lung treatment with dicumarol (NQO1 inhibitor) decreased the rate of DQH_2 efflux by >95% during the infusion of DQ at the highest concentration. This is consistent with NQO1 being the dominant

Journal of Applied Physiology, Vol 111, No. 1 (July 2011): pg. 95-107. DOI.

reductase of DQ on passage through the pulmonary circulation of normoxic, hyper-60, and hyper-85 lungs.[5,6]

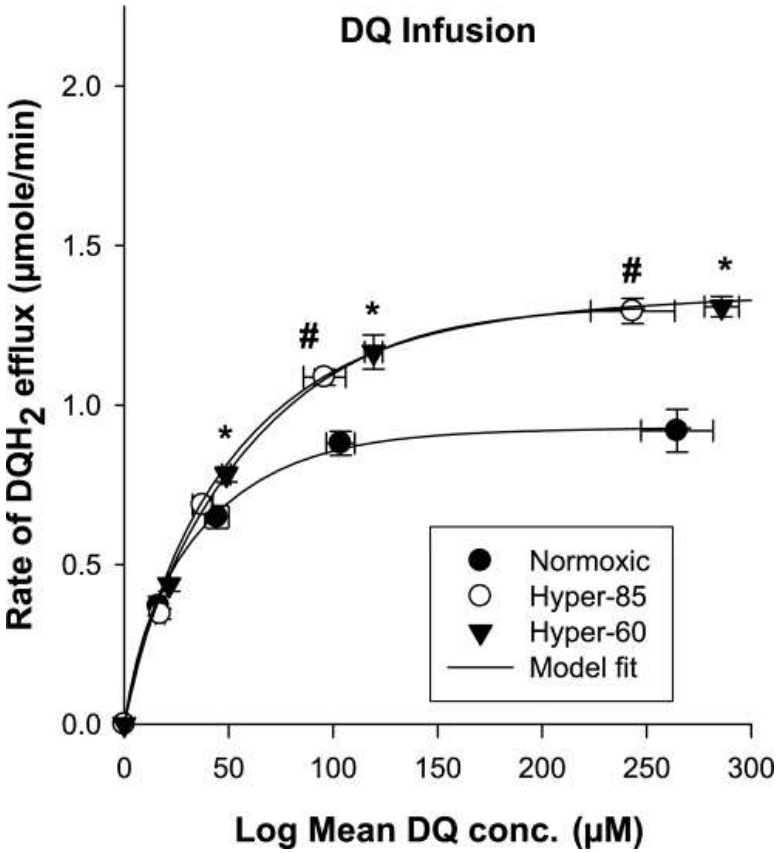

Fig. 2. The relationship between the steady-state rate of durohydroquinone (DQH_2) efflux and the log mean duroquinone (DQ) concentrations, which are effective intravascular DQ concentrations during DQ arterial infusion, for normoxic lungs (n = 4), hyper-85 lungs (n = 5), and hyper-60 lungs (n = 5). Values are means ± SE. The solid lines are model fits to the mean values of the data. *Hyper-60 rates significantly different from the normoxic rates at the same log mean DQ concentrations; # hyper-85 rates significantly different from the normoxic rates at the same log mean DQ concentrations ($P < 0.05$).

To evaluate the capacity of the lung to oxidize DQH_2, we measured the steady-state rate of DQ efflux during DQH_2 infusion in the presence of dicumarol to inhibit DQ reduction (Fig. 3). For hyper-60 and hyper-85 lungs, the rates of DQ efflux during DQH_2 infusion at the two highest concentrations were 40% higher than in normoxic lungs (Fig. 3). For all three groups of lungs, treatment with antimycin A (complex III inhibitor) decreased the rate of DQ efflux to nearly zero during DQH_2 infusion at the highest concentration. This is consistent with DQH_2 oxidation on passage through normoxic and hyperoxic lungs

occurring predominately via the hydroquinone oxidase-cytochrome *c* reductase activity of complex III.[5,6]

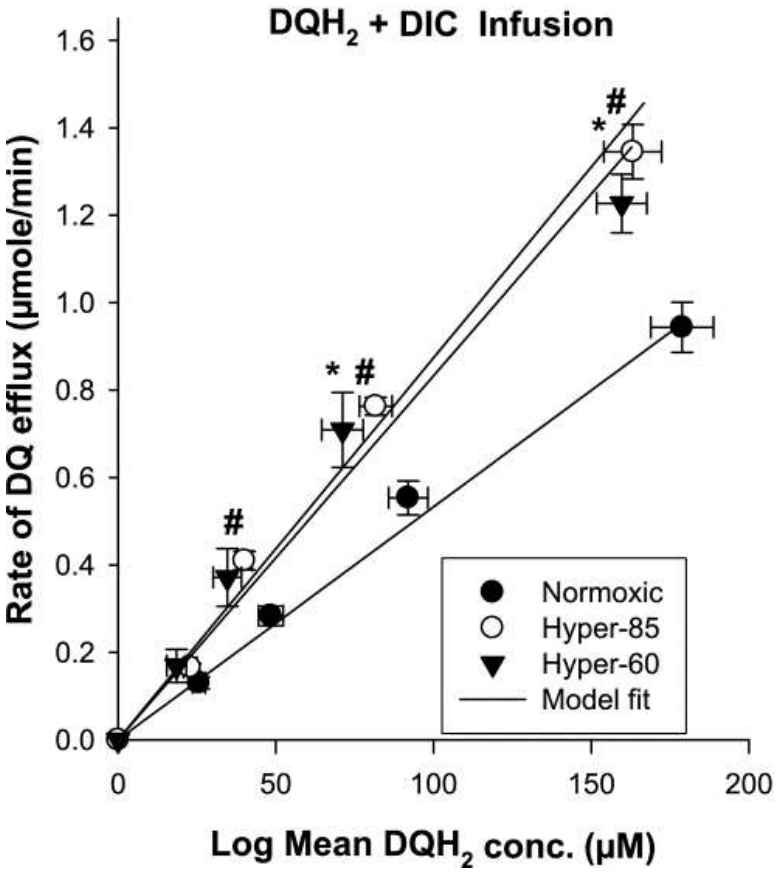

Fig. 3. The relationship between the steady-state rate of DQ efflux and the log mean DQH_2 concentrations, which are the effective intravascular DQH_2 concentrations during DQH_2 arterial infusion in the presence of dicumarol (DIC, 400 µM), for normoxic lungs (n = 6), hyper-85 lungs (n = 6), and hyper-60 lungs (n = 4). Values are means ± SE. The solid lines are model fits to the mean values of the data. *Hyper-60 rates significantly different from the normoxic rates at the same log mean DQH_2 concentrations; # hyper-85 rates significantly different from the normoxic rates at the log mean DQH_2 concentrations ($P < 0.05$).

To evaluate the effect of rat exposure to hyper-60 or hyper-85 on NQO1-mediated DQ reduction, the rate of DQH_2 efflux during DQ infusion was measured in the presence of antimycin A to inhibit DQH_2 oxidation (Fig. 4). As expected, antimycin A increased the rates of DQH_2 efflux (Figs. 2 and and 4) over the range of infused DQ concentrations. Moreover, both O_2 levels increased the rate of DQH_2 efflux during DQ infusion at the two highest concentrations in the presence of antimycin A compared with normoxic lungs, but the

Journal of Applied Physiology, Vol 111, No. 1 (July 2011): pg. 95-107. DOI.

increase was larger for the hyper-85 lungs (52%) than for the hyper-60 lungs (23%) (Fig. 4).

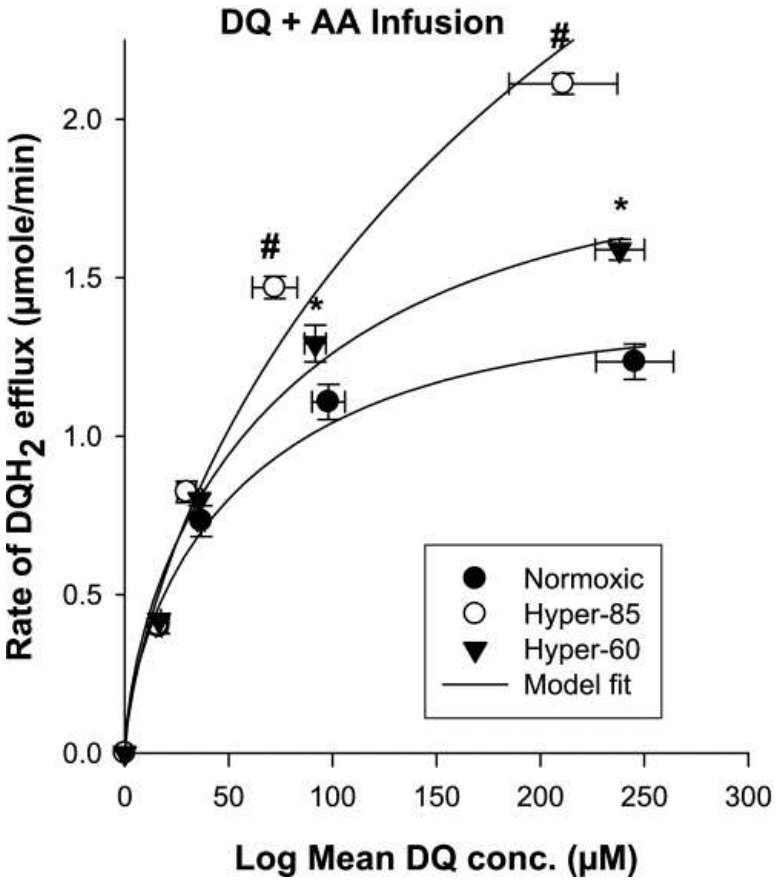

Fig. 4. The relationship between the steady-state rate of DQH_2 efflux and the log mean DQ concentrations, which are the effective intravascular DQ concentrations during DQ arterial infusion in the presence of antimycin A (AA, 10 µM), for normoxic lungs (n = 5), hyper-85 lungs (n = 5), and hyper-60 lungs (n = 5). Values are means ± SE. The solid lines are model fits to the mean values of the data. *Hyper-60 rates significantly different from the normoxic rates at the same log mean DQ concentrations; # hyper-85 rates significantly different from the normoxic rates at the same log mean DQ concentrations ($P < 0.05$).

To evaluate the effect of rat exposure to hyper-85 or hyper-60 on mitochondrial complex III-mediated DQH_2 oxidation, the rate of DQ efflux during DQH_2 infusion was measured in the presence of dicumarol and rotenone. Again, rotenone was added to minimize competition between DQH_2 and reduced endogenous coenzyme Q_9 hydroquinone (CoQ_9H_2) for oxidation via complex III. Figure 5 shows that, for hyper-85 lungs, the steady-state rates of DQ efflux during DQH_2 infusion at the two highest concentrations in the presence of dicumarol plus rotenone were ~30% higher than those in normoxic

Journal of Applied Physiology, Vol 111, No. 1 (July 2011): pg. 95-107. DOI.

lungs. For all three groups of lungs, the rate of DQ efflux during DQH_2 infusion at the highest concentration in the presence of antimycin A along with dicumarol and rotenone was virtually zero. This further supports that complex III is the dominant site for DQH_2 oxidation on passage through the pulmonary circulation of all three groups of lungs.

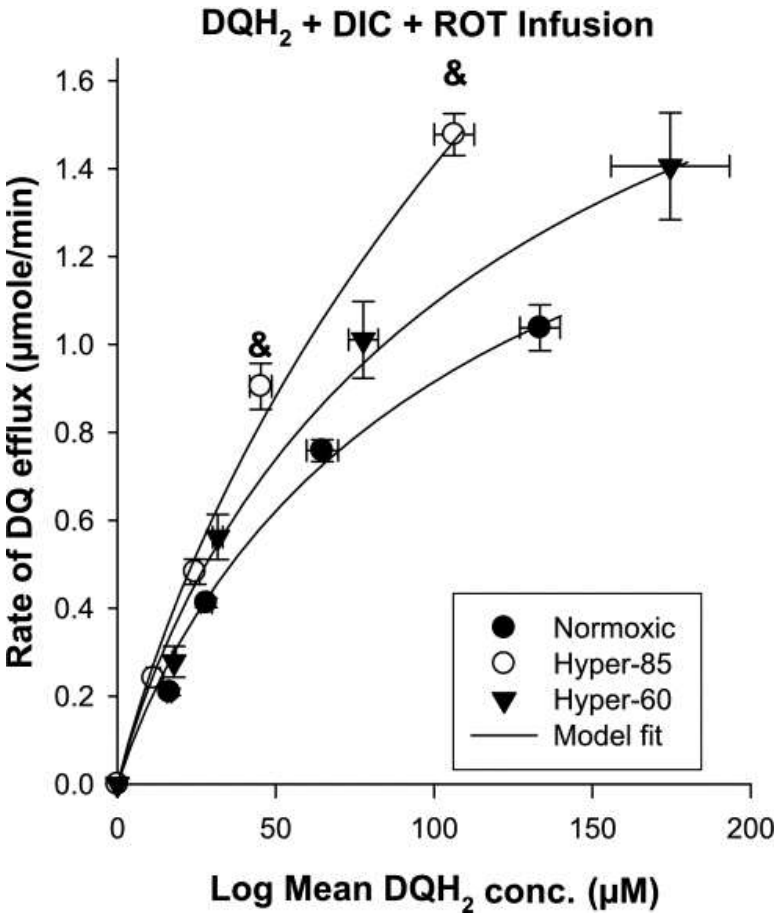

Fig. 5. The relationship between the steady-state rate of DQ efflux and the log mean DQH_2 concentrations, which are the effective intravascular DQH_2 concentrations during DQH_2 arterial infusion in the presence of DIC (400 µM) plus rotenone (ROT, 20 µM), for normoxic lungs (n = 4), hyper-85 lungs (n = 4), and hyper-60 lungs (n = 4). Values are means ± SE. The solid lines are model fits to the mean values of the data. & Hyper-85 rates significantly different from the normoxic rates at the same log mean DQH_2 concentrations ($P < 0.05$).

Table 2 shows that rat exposure to hyper-85 increased NOQ1 homogenate activity per lung by 72%, but had no significant effect on NQO1 activity per milligram of protein. Exposure to hyper-60, on the other hand, had no significant effect on NQO1 activity in homogenate per lung or per milligram of protein.

Journal of Applied Physiology, Vol 111, No. 1 (July 2011): pg. 95-107. DOI.

Table 2. Lung homogenate NQO1 activity

	Homogenate NQO1 Activity	
	μmol · min^{-1} · lung^{-1}	**nmol · min^{-1} · mg protein^{-1}**
Normoxic	26.48 ± 1.67	670 ± 80
Hyper-60	34.75 ± 1.98	737 ± 63
Hyper-85	45.55 ± 4.74*†	538 ± 43

Values are means ± SE; *n* = 7, 10, and 7 for normoxic, hyper-60, and hyper-85 lungs, respectively. NQO1, NAD(P)H:quinone oxidoreductase 1. Significantly different from the corresponding * normoxic and † hyper-60 values, $P < 0.05$.

We also measured the activities of mitochondrial complexes I and IV in lung tissue homogenates. Table 3 shows that mitochondrial complex I activities per milligram protein were ~50% lower in P2 fractions derived from hyper-85 and hyper-60 lungs than normoxic lungs. Complex IV activity per milligram protein increased in only hyper-85 lung homogenates by 90% compared with normoxic lungs (Table 3).

Table 3. Mitochondrial complexes I and IV activities measured in P2 fractions of lung homogenates

	Complex I Activity	**Complex IV Activity**
Normoxic	13.18 ± 2.31	231.8 ± 15.9
Hyper-60	6.49 ± 0.84*	201.8 ± 45.8
Hyper-85	6.78 ± 1.24*	439.3 ± 50.8*

Values are means ± SE in nmol · min^{-1} · mg protein^{-1}; for complexes I and IV activities, *n* = 5, 5, and 7 for normoxic, hyper-60, and hyper-85 lungs, respectively. *Significantly different from the corresponding normoxic value, $P < 0.05$.

Table 4 shows that total glutathione content (oxidized plus reduced glutathione) per lung and per gram of dry lung weight increased by 101 and 20%, respectively, in hyper-85 lungs only compared with normoxic lungs.

Table 4. Total lung glutathione (GSH + GSSG) content

	(GSH + GSSG), μmol/lung	**(GSH + GSSG), μmol/g dry wt**
Normoxic	2.34 ± 0.17	10.23 ± 0.55
Hyper-60	3.09 ± 0.14	11.96 ± 0.77
Hyper-85	4.70 ± 0.39*†	12.21 ± 0.47*

Values are means ± SE; *n* = 8, 5, and 7 for normoxic, hyper-60, and hyper-85 lungs, respectively. GSH, reduced glutathione; GSSG oxidized glutathione. Significantly different from the corresponding * normoxic and † hyper-60 values, $P < 0.05$.

Journal of Applied Physiology, Vol 111, No. 1 (July 2011): pg. 95-107. DOI.

Data analysis.

The data in Figs. 22–5 are the net result of multiple factors, including *1*) DQ and DQH_2 interactions with competing nonlinear tissue redox processes; *2*) DQ and DQH_2 interactions with protein (i.e., BSA) in the vascular space; and *3*) capillary perfusion kinematics [i.e., a heterogeneous distribution, $h_c(t)$, of capillary transit times]. Thus, for quantitative interpretation of the data in Figs. 22–5, we utilized a whole lung kinetic model consisting of a capillary region that accounts for DQ and DQH_2 tissue and vascular interactions and conducting arteries and veins.[52] The capillary region has a $h_c(t)$.[5,6,9] The model was used to estimate parameters descriptive of the activities of NQO1 and complex III in the isolated perfused lung from the data in Figs. 22–5.

The capillary region is modeled as parallel noninteracting capillary elements with transit times distributed according to $h_c(t)$.[8] Figure 6 shows a single capillary element consisting of a vascular region and its surrounding lung tissue region with volumes V_c (ml) and V_e (ml), respectively. Within the vascular region, DQ and DQH_2 participate in nonspecific and rapidly equilibrating interactions with the perfusate albumin (BSA). The free (i.e., not BSA bound) vascular concentrations of DQ and DQH_2 can freely permeate the tissue region from the vascular region. Within the tissue region, DQ is reduced via NQO1, and DQH_2 is oxidized via mitochondrial complex III. This reduction and oxidation are assumed to follow Michaelis-Menten kinetics, where V_{max} and K_m represent the maximum reduction or oxidation rate and Michaelis-Menten constant, respectively. All nonspecific DQ and DQH_2 interactions are assumed to follow the law of mass action. The above assumptions were incorporated into a differential equation model presented in the appendix.

Journal of Applied Physiology, Vol 111, No. 1 (July 2011): pg. 95-107. DOI.

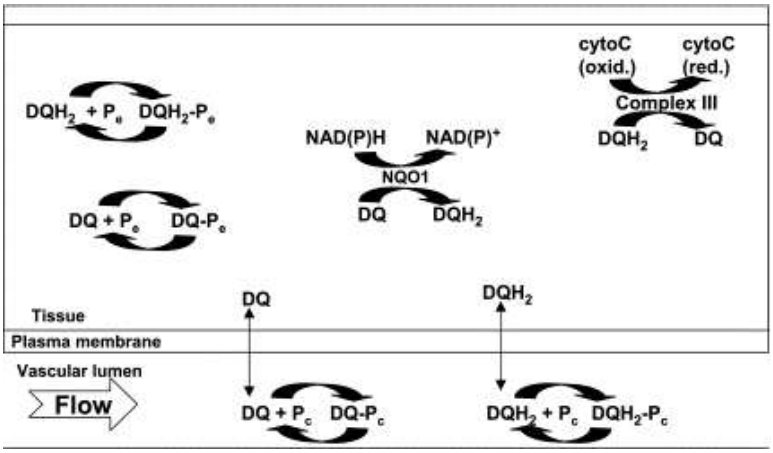

Fig. 6. A schematic representation of the vascular and lung tissue interactions of DQ and DQH_2 in a single capillary element consisting of a vascular region and its surrounding tissue region. Within the vascular region, DQ and DQH_2 participate in nonspecific and rapidly equilibrating interactions with the perfusate BSA, P_c. Within the tissue region, DQ is reduced via NAD(P)H:quinone oxidoreductase 1 (NQO1), and DQH_2 is oxidized via complex III. Also within the tissue volume, DQ and DQH_2 undergo nonspecific rapidly equilibrating interactions with lung tissue, P_e. CytoC (oxid.) and cytoC (red.) are the oxidized and reduced forms of cytochrome *c*, respectively.

Estimation of model parameters.

The unknown model parameters under steady-state conditions (see appendix) are V_{max1} (μmol/min) and V_{max2} (μmol/min), the respective maximum rates for DQ reduction via NQO1 and DQH_2 oxidation via complex III; K_{m1a} (μM) and K_{m2a} (μM), the apparent Michaelis-Menten constants for NQO1-mediated DQ reduction and complex III-mediated DQH_2 oxidation, respectively; and k_{ox} (ml/min), the tissue-mediated DQH_2 oxidation rate on passage through the pulmonary circulation in the absence of rotenone.

The values of these parameters for each of the three groups of lungs were estimated using the following approach. First, the values of V_{max1} and K_{m1a}, parameters descriptive of NQO1-mediated DQ reduction, were determined. This was done by fitting the steady-state solution of the lung model to the steady-state rates of DQH_2 efflux during DQ infusion in the presence of antimycin A (Fig. 4), which corresponded to setting V_{max2} to zero in *Eqs. A1* and *A2*. The estimated values of these model parameters are given in Table 5. Rat exposure to hyper-85 for 7 days increased V_{max1} by ~200%. The estimated values of V_{max1} for hyper-60 lungs tended to be higher than those for normoxic lungs, but the mean difference was not significant (one-way

Journal of Applied Physiology, Vol 111, No. 1 (July 2011): pg. 95-107. DOI.

ANOVA). For all three groups of lungs, the estimated value of K_{m1a} was 1 μM, which was the lower bound set for this parameter in the least squares fitting procedure. K_{m1a} is an intensive property of the enzyme and hence would be expected to be the same for all three groups of lungs.

Table 5. Values of model parameters descriptive of NQO1-mediated DQ reduction in normoxic and hyperoxic lungs estimated from the steady-state DQH_2 efflux rates during DQ infusion in the presence of antimycin A

	V_{max1}		
	μmol/min	**μmol · min^{-1} · g dry wt^{-1}**	**K_{ma1}, μM**
Normoxic	1.38 ± 0.07	6.4 ± 0.3	1.0
Hyper-60	1.84 ± 0.06	7.8 ± 0.5	1.0
Hyper-85	4.11 ± 0.39*†	10.8 ± 0.7*†	1.0

Values are means ± SE; n = 5 for all three groups. V_{max1}, maximum duroquinone (DQ) reduction rate; K_{ma1}, apparent Michaelis-Menten constant. DQH2, durohydroquinone. Significantly different from * normoxic and † hyper-60 values, $P < 0.05$.

For a given lung, parameters descriptive of complex III-mediated DQH_2 oxidation (V_{max2} and K_{m2a}) were estimated by fitting the steady-state solution of the organ model to the rates of DQ efflux during DQH_2 infusion in the presence of dicumarol and rotenone (Fig. 5), with V_{max1} set to zero in *Eqs. A1* and *A2* to account for the presence of dicumarol. Results in Table 6 show that exposure to hyper-85 increased V_{max2} by ~180%, compared with normoxic lungs, with no significant effect on K_{m2a}. The estimated values of V_{max2} and K_{m2a} for hyper-60 lungs were not significantly different from those estimated for normoxic lungs.

Table 6. Values of model parameters descriptive of complex III-mediated DQH_2 oxidation in normoxic and hyperoxic lungs estimated from the steady-state DQ efflux rates during DQH_2 infusion in the presence of dicumarol plus rotenone

	V_{max2}		
	μmol/min	**μmol · min^{-1} · g dry wt^{-1}**	**K_{ma2}, μM**
Normoxic	1.67 ± 0.10	8.7 ± 0.7	42 ± 2
Hyper-60	2.07 ± 0.09	8.8 ± 0.5	38 ± 6
Hyper-85	4.65 ± 0.36*†	13.6 ± 1.8*†	36 ± 11

Values are means ± SE. n = 4 for all three groups. V_{max2}, maximum DQH_2 oxidation rate; K_{ma2}, apparent Michaelis-Menten constant. Significantly different from * normoxic and † hyper-60 values, $P < 0.05$.

Journal of Applied Physiology, Vol 111, No. 1 (July 2011): pg. 95-107. DOI.

In the absence of rotenone (complex I inhibitor), DQH_2 competes with CoQ_9H_2 for oxidation via complex III. This competition explains the observation that the rates of DQ efflux during DQH_2 infusion in the presence of dicumarol alone are lower than those in the presence of dicumarol plus rotenone (Figs. 3 and and 5). Moreover, the steady-state DQ efflux rates during DQH_2 infusion in the presence of dicumarol alone appear to follow linear kinetics for the range of infused DQH_2 concentrations studied (Fig. 3). Thus, in the absence of rotenone, V_{max2} and K_{m2a} in *Eqs. A1* and *A2* (appendix) are substituted for with k_{ox} (*Eqs. A3* and *A4*). To put k_{ox} in perspective, if one were to assume Michaelis-Menten kinetics for DQH_2 oxidation in the presence of dicumarol alone, k_{ox} would be the ratio of the maximum oxidation rate over the Michaelis-Menten constant.

The value of k_{ox} was estimated by fitting the model, with V_{max1} set to zero in *Eqs. A3* and *A4*, to the steady-state rates of DQH_2 efflux during DQ infusion in the presence of dicumarol (Fig. 3). Table 7 shows that rat exposure to hyper-60 or hyper-85 for 7 days increased the estimated value of k_{ox} by ~70 and ~140%, respectively, compared with normoxic lungs.

Table 7. Value of model parameter descriptive of the DQH_2 oxidation capacity in normoxic and hyperoxic lungs estimated from the steady-state DQ efflux rates during DQH_2 infusion in the presence of dicumarol

	k_{ox}	
	ml/min	**ml · min^{-1} · g dry wt^{-1}**
Normoxic	6.38 ± 0.60	27.6 ± 2.9
Hyper-60	10.84 ± 1.25*	43.1 ± 4.0*‡
Hyper-85	15.16 ± 1.58*†	35.0 ± 8.4

Values are means ± SE; n = 6, 4, and 6 for normoxic, hyper-60, and hyper-85 lungs, respectively. k_{ox}, rate of DQH_2 oxidation on passage through the pulmonary circulation. Significantly different from * normoxic, † hyper-60, and ‡ hyper-85 values, $P < 0.05$.

A second estimate of the values of V_{max1} and K_{m1a} for normoxic and hyperoxic lungs was obtained by fitting the steady-state organ model solution to the steady-state rates of DOH_2 efflux during DQ infusion in the absence of inhibitors (Fig. 2), with k_{ox} in *Eqs. A3* and *A4* set to the mean values in Table 7. The estimated values of V_{max1} for hyper-60 and hyper-85 lungs were ~80 and 140% higher than that estimated for normoxic lungs, respectively (Table 8).

Journal of Applied Physiology, Vol 111, No. 1 (July 2011): pg. 95-107. DOI.

Table 8. Values of model parameters descriptive of NQO1-mediated DQ reduction in normoxic and hyperoxic lungs estimated from the steady-state DQH_2 efflux rates during DQ infusion

	V_{max1}		
	μmol/min	**μmol · min^{-1} · g dry wt^{-1}**	**K_{ma1}, μM**
Normoxic	1.46 ± 0.10	7.2 ± 0.8	4.4 ± 1.4
Hyper-60	2.64 ± 0.08*	11.8 ± 0.5*	12.5 ± 2.1*‡
Hyper-85	3.52 ± 0.12*†	10.1 ± 0.6*	6.4 ± 1.6

Values are means ± SE; n = 4, 5, and 5 for normoxic, hyper-60, and hyper-85 lungs, respectively. k_{ox} was set to the mean value in Table 5. Significantly different from * normoxic, † hyper-60, and ‡ hyper-85 values, $P < 0.05$.

For normoxic and hyper-85 lungs, the values of V_{max1} in Table 8 vs. Table 5, i.e., estimated from the steady-state rates of DQH_2 efflux during DQ infusion in the absence or presence, respectively, of antimycin A were not significantly different. This is consistent with the hypothesis that the dominant effect of antimycin A is on complex III-mediated DQH_2 oxidation. However, for hyper-60 lungs, the estimated values of V_{max1} were statistically different for the two approaches.

Discussion

The results of the present study demonstrate that rat exposure to hyper-85 vs. hyper-60 differentially altered the lung tissue complex III and IV activities, and GSH content, but had similar effects on NQO1 and complex I activities. In hyper-85 rats, the capacity of V_{max1} and V_{max2} increased by 140 and 180%, respectively, on passage through the pulmonary circulation. However, hyper-60 increased V_{max1} by 80%, with no effect on V_{max2}. Additional results demonstrate that hyper-60 and hyper-85 decreased complex I activity by ~50%, and that hyper-85, but not hyper-60, increased complex IV activity and GSH tissue content by 90 and 20%, respectively.

In addition to increasing V_{max1} and V_{max2}, rat exposure to hyper-85 increased lung dry weight (Table 1), presumably due to a large increase in the number of interstitial cells.[24,25] This brought into question whether the estimated increase in these extensive kinetic parameters was simply the result of an increase in tissue mass (i.e., more cells). As shown in Tables 6 and and 8, the increase in the dry weight of hyper-85 lungs cannot account for all of the increase in the

Journal of Applied Physiology, Vol 111, No. 1 (July 2011): pg. 95-107. DOI.

values of V_{max1} and V_{max2}, since the values per gram of dry lung are, respectively, 40 and 56% higher than corresponding values for normoxic lungs. The above results suggest that rat exposure to hyper-85 induced an increase of 40 and 56% in the lung activities of NQO1 and complex III per gram of dry lung weight, respectively.

For normoxic and hyper-85 lungs, the estimates of V_{max1} obtained using two independent data sets, i.e., DQH_2 efflux rates during DQ infusion in the absence or presence of antimycin A, are not significantly different (Tables 5 and and 8). However, for hyper-60 lungs, the difference in these values is 42%. One reason for this difference might be that treatment of hyper-60 lungs with antimycin A not only inhibited complex III-mediated DQH_2 oxidation, but also partially inhibited NQO1-mediated DQ reduction or other DQ reductase(s).[68] In addition to inhibiting DQH_2 oxidation, antimycin A would be expected to inhibit ATP production via oxidative phosphorylation. This impairment to ATP production could stimulate glycolysis[1–3, 58] This, in turn, would divert glucose-6-phosphate from the pentose phosphate pathway, the main source of NADPH for NOQ1.[13] This suggests that, for hyper-60 lungs, the rate of NAPDH production in the presence of antimycin A may not be sufficient to maintain the maximum capacity of NQO1 for DQ reduction that is measurable in the absence of antimycin A (Figs. 2 and and4). This explanation is consistent with previous studies that demonstrated that rat exposure to hyper-85, but not hyper-60, increased lung activities of glucose transporters, hexokinase, and glucose-6-phosphate dehydrogenase (G-6-PHD) compared with normoxic lungs (Table 9).[1–3,40,64]

Table 9. Summary of the effect of rat exposure to hyper-60 or hyper-85 for 7 days on cell surface, cytosolic, and mitochondrial enzymes

	Hyper-60 for 7 days, %	**Hyper-85 for 7 days, %**	**Reference No.**
NQO1 per g dry wt	+64	+40	Present study
Complex III per g dry wt	NS	+56	Present study
Complex I per mg protein	−51	−49	Present study
Complex IV per mg protein	NS	+90	Present study
ACE	NS	−57	Present study
k_{ox} per g dry wt	+56	NS	Present study
Lung glutathione content per g dry wt	NS	+20	Present Study

Journal of Applied Physiology, Vol 111, No. 1 (July 2011): pg. 95-107. DOI.

	Hyper-60 for 7 days, %	Hyper-85 for 7 days, %	Reference No.
G-6-PDH per g dry wt	NS	+68	40
Hexokinase per mg protein	NA	+44	2
g-Glutamyltransferase per μU/mg	NS	+220	67

G-6-PDH, glucose-6-phosphate dehydrogenase. NS, not significant; NA, not available.

Figure 7 shows high correlation between homogenate NQO1 activity and the capacity (V_{max1}) of NQO1-mediated DQ reduction in normoxic, hyper-60, and hyper-85 lungs. However, the increase in V_{max1} is larger than the increase in NQO1 homogenate activity in hyper-60 and hyper-85 lungs. One reason for this difference may be that hyperoxia-induced changes in key aspects of the intact lung environment that regulate NQO1 activity (e.g., availability of electron donors and their accessibility to the enzyme) are not preserved in lung homogenates.[6] Another reason may be that other dicumarol-inhibitable reductase(s) besides NQO1 contribute to DQ reduction.[37,68,72] Although NQO1 is predominantly a cytosolic enzyme (>90%),[55] noncytosolic NQO1 activity has been previously reported.[11,37,63] Thus another reason for the above difference may be that these O_2 levels induced an increase in NQO1 activity in the noncytosolic fraction of the lung tissue, which was not preserved in the tissue homogenate used for the NQO1 assay.

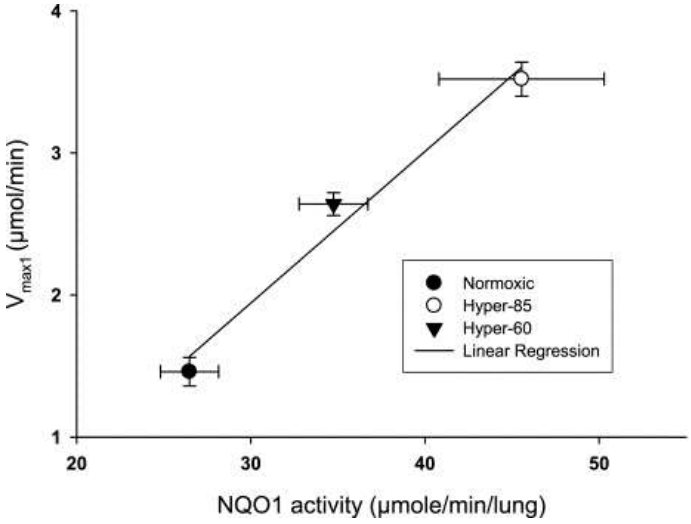

Fig. 7. Relationship between total NQO1 activity in lung tissue homogenates (Table 2) and the capacity (V_{max1}) of NQO1 mediated DQ reduction (Table 8) on passage through the pulmonary circulation of normoxic, hyper-60, or hyper-85 lungs. Values are means ± SE. Solid line is linear model fit (r^2 = 0.975).

Several studies have evaluated the role of NQO1 in protection against pulmonary O_2 toxicity.[20,70] Whitney and Frank[70] found that the induction of NQO1 did not significantly improve the survivability of adult rats exposed to lethal O_2 levels. On the other hand, Cho et al.[20] showed that mice deficient in the transcription factor Nrf2, which is involved in the induction of phase II enzymes, including NQO1, had significantly lower lung NQO1 mRNA expression and were significantly more sensitive to hyperoxia (>95% O_2 for 72 h) than wild-type mice. Previously, our laboratory demonstrated that rat exposure to hyper-85 for 21 days, but not for 2 days, increased the capacity of NQO1-mediated DQ reduction on passage through the lungs and suggested a potential role for NQO1 in rat tolerance of 100% O_2 toxicity.[6,9] One of the objectives of this study was to determine whether rat exposure to hyper-60 or hyper-85 has a differential effect on the lung activity of NQO1. The results of this study reveal that both hyperoxic O_2 levels increase NQO1 activity in the isolated perfused lung.

The difference in the rate of DQ efflux during DQH_2 infusion in the presence of dicumarol (Fig. 3) compared with that in the presence of dicumarol plus rotenone (Fig. 5) is consistent with competition between infused DQH_2 and complex I-generated CoQ_9H_2 for complex III-mediated oxidation. Hence, this difference is a measure of the capacity of complex I for generating reducing equivalent (CoQ_9H_2) and of lung tissue rotenone-sensitive O_2 consumption. Previously, our laboratory estimated the rate of rotenone-sensitive O_2 consumption in normoxic lungs to be ~1.4 μmol·min^{-1}·g dry lung wt^{-1}.[5] This rate (which needs to be multiplied by two for comparison with the difference in DQ efflux rate in Fig. 8) is comparable with the maximum difference in DQ efflux rate (~2.4 μmol·min^{-1}·g dry lung wt^{-1}) in normoxic lungs (Fig. 8).

Journal of Applied Physiology, Vol 111, No. 1 (July 2011): pg. 95-107. DOI.

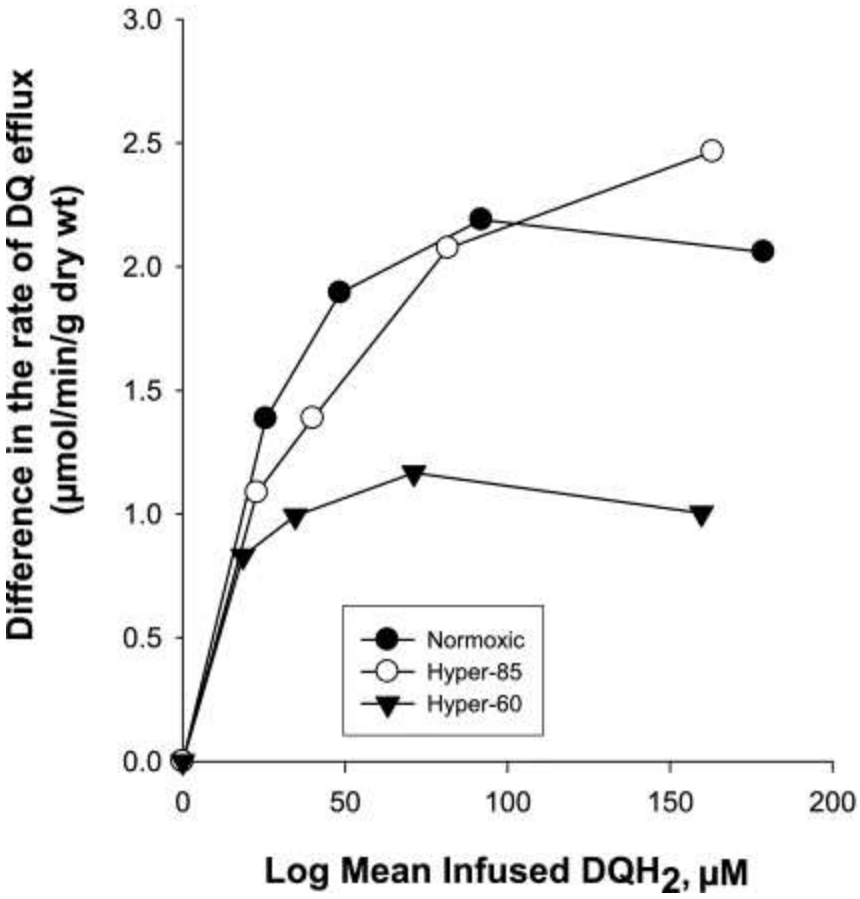

Fig. 8. The relationship between the difference in steady-state rates (normalized to dry lung weight) of DQ efflux and the log mean DQH_2 concentrations during DQH_2 arterial infusion in the presence of DIC plus ROT (Fig. 5) and DIC alone (Fig. 3), for normoxic lungs, hyper-85 lungs, and hyper-60 lungs. Model-based interpolation was used to determine the rates of DQ efflux in the presence of DIC plus ROT (Fig. 5) at the same log mean DQH_2 concentrations as in Fig. 3.

For hyper-85 lungs, the difference in the DQ efflux rate in the presence of dicumarol or dicumarol plus rotenone (Fig. 8) was comparable to that for normoxic lungs. However, for hyper-60 lungs, the difference was ~50% smaller than that for normoxic lungs (Fig. 8). This suggests a potential decrease in the capacity of complex I for generating CoQ_9H_2 in hyper-60 lungs compared with normoxic and hyper-85 lungs. This could be due to a decrease in lung tissue complex I activity and/or decrease in the rate of the metabolic coenzyme NADH supplied to complex I. Table 3 shows that exposure to hyper-85 or hyper-60 decreased lung complex I activity (per milligram of protein) by ~50%. This decrease appears to have no significant effect on the capacity of complex I for generating CoQ_9H_2 in hyper-85 lungs (Fig. 8),

Journal of Applied Physiology, Vol 111, No. 1 (July 2011): pg. 95-107. DOI.

suggesting a possible increase in the rate of NADH supplied to complex I to compensate for the decrease in complex I activity. This would be consistent with an increase in tissue activities of glucose transporters and hexokinase in hyper-85 lungs.[3] For hyper-60 lungs, the decrease in complex I activity (Table 3) is proportional to the decrease in the rate of complex I-generated CoQ_9H_2 (Fig. 8).

Ratner et al.[53] demonstrated that exposure of neonatal mice to hyperoxia (75% O_2 for 72 h) decreases complex I activity by ~70%, and that this decrease compromises mitochondrial oxidative phosphorylation and contributes to alveolar development arrest. Based on these results, they concluded that the decrease in complex I plays a key role in lung O_2 toxicity. In the present study, exposure to hyper-60 or hyper-85 decreased complex I activity by ~50%. However, for hyper-85 lungs, the effect of this decrease on oxidative phosphorylation may have been countered by an increase in the lung activities of glucose transporters and hexokinase upstream from complex I,[2] and by an increase in the activities of complexes III and IV downstream from complex I (Table 9). Additional studies would be needed to evaluate the effect of this depression in complex I activity on the mitochondrial rate of ATP production.

Rat exposure to hyper-85, but not hyper-60, increased lung tissue activities of complexes III and IV by 56 and 90%, respectively. Again, this may be a compensatory mechanism to counter the potential effects of the depression in complex I activity on mitochondrial ATP production.[28] The increase in lung complexes III and IV activities could also be a means of decreasing ROS production at complexes I and III, since the higher the respiration rate, the less time the electrons are delayed at critical leakage sites, such as complexes I and III.[18,45] Campian et al.[18] showed that an O_2-tolerant strain of HeLa cells had a higher complex IV activity and a lower rate of mitochondrial ROS production compared with wild-type HeLa cells. Furthermore, they showed that inhibiting the complex IV activity of these O_2-tolerant cells increased their rate of mitochondrial ROS production and increased their sensitivity to hyperoxia. Based on these results, they attributed the O_2 tolerance of these cells to their higher than normal complex IV activity, which results in a tighter coupling of the electron transport chain and a lower rate of mitochondrial ROS formation.[18] Additional studies would be needed to evaluate the effect of the measured

Journal of Applied Physiology, Vol 111, No. 1 (July 2011): pg. 95-107. DOI.

increase in tissue complexes III and IV activities of hyper-85 lungs on mitochondrial rates of ATP production and ROS formation and to determine the role of complexes III and IV in rat tolerance of 100% O_2 toxicity.

Previous studies have suggested a role for the pentose phosphate pathway in rat tolerance of 100% O_2.[64] This pathway provides reducing equivalents (NADPH) for the glutathione redox cycle and for the synthesis of cellular components needed for repair mechanisms.[64] Tierney et al.[64] demonstrated an increase in the activity of the enzyme G-6-PHD in lungs of rats, but not mice, exposed to hyper-85. Hayatdavoudi et al.[40] demonstrated an increase in G-6-PHD activity in lungs of hyper-85 rats, but not hyper-60 rats. The results of the present study demonstrate an increase in lung tissue total glutathione (GSH) content per milligram of protein in hyper-85 lungs, but not hyper-60 lungs, compared with normoxic lungs (Table 4). This result is consistent with an increase in γ-glutamyltransferase activity in tissue homogenates of hyper-85 lungs, but not hyper-60 lungs, reported by Van Klaveren et al.[67] (Table 9). This enzyme is important for the uptake of substrates for intracellular GSH synthesis. However, in the same study, Van Klaveren et al. reported no increase in GSH level in hyper-85 tissue homogenates per milligram protein, which is different from the results in the present study.[67] This difference may be due to differences in rat strains (Wistar vs. Sprague-Dawley) and/or the methods used to measure tissue GSH content. The increase in GSH content in hyper-85 lung homogenates measured in the present study is potentially important, since GSH is the major mechanism for scavenging H_2O_2 in endothelial cells, and since H_2O_2 is the most cytotoxic ROS in endothelial cells, which are a primary target of lung O_2 toxicity.[62]

For hyper-60 lungs, the decrease in complex I activity did not stimulate changes in substrate availability, activities of complexes III and IV, GSH content, and/or G-6-PDH activity to counter the potential effect of a 50% depression in complex I activity on mitochondrial rates of ATP production and ROS formation, and on GSH redox cycle. This could make hyper-60 lung cells susceptible to further injury by a hyperoxia-induced increase in the rate of ROS formation. The increase in the susceptibility of hyper-60 rats to 100% O_2 toxicity could also be due to changes in other cellular processes. For instance, hyper-60

rates are more susceptible to mechanical ventilation injury than are normoxic rats.[40] Additional studies would be needed to evaluate the effect of rat exposure to hyper-60 on lung tissue rates of mitochondrial ROS formation and ATP production.

Since mice do not acquire tolerance of 100% O_2 following exposure to hyper-85,[19,26] a lack of increase in complexes III and IV activities and GSH content in lungs of mice exposed to hyper-85 would provide further evidence for the potential role of these redox processes in rat tolerance of 100% O_2. However, the inability of mice to acquire tolerance of 100% O_2 could also be due to changes in other cellular processes.

Rat tolerance of 100% O_2 can be induced, not only by preexposing rats to hyper-85 for 7 days, but also by other experimental means, including rat preexposure to 95% O_2 for 48 h, followed by a 24-h "rest period" in room air or 50–70% O_2 (hyper-95).[33] Thus another approach to providing additional support for the potential role of complexes III and IV and GSH redox cycle in rat tolerance of 100% O_2 would be to demonstrate that their activities also increase in lungs of rats exposed to hyper-95.

Because patients requiring high O_2 come with differing tolerances of hyperoxia based on genetics, preconditioning, or other factors, real-time information that permits clinicians to determine which patients are developing toxicity is invaluable.[36] The identified changes in complexes III and IV and GSH content may provide targets for clinical biomarker imaging (e.g., SPECT, PET, MRI) to detect tolerance of, or susceptibility to, high O_2. For instance, the ability of lung tissue to increase its capacity to generate GSH or increase its activities of complexes III and IV may be indicative of the ability of a critically ill patient to tolerate sustained exposure to O_2 at high fractions. In contrast, a patient with the same O_2 requirement and no increase in GSH content or activities of complexes III and IV could be at a much higher risk for irreversible lung injury. In this case, the patient with evidence of enhanced susceptibility to hyperoxia should be a candidate for therapies that otherwise would not be employed because of toxicity, e.g., higher positive end-expiratory pressure, acceptance of lower arterial O_2 tension, extracorporeal membrane oxygenation, and moderate hypothermia.

Journal of Applied Physiology, Vol 111, No. 1 (July 2011): pg. 95-107. DOI.

In conclusion, the results demonstrate that NQO1 activity increased in both hyper-60 and hyper-85 lungs, whereas complex III activity increased in hyper-85 lungs only. This increase, along with the increase in complex IV activity, substrate availability, and G-6-PHD in hyper-85 lungs, could be to counter the effects that the depression in complex I activity might have on mitochondrial ATP production and ROS formation, and on GSH redox cycle, and hence be important to rat tolerance of 100% O_2. The results demonstrate the utility of these two hyperoxic models and indicator dilution methods for furthering understanding of the pathogenesis of lung O_2 toxicity and for providing insights into the underlying mechanisms of rat tolerance of and susceptibility to 100% O_2.

Grants

This work was supported by National Heart, Lung, and Blood Institute Grant HL-24349 and the Department of Veterans' Affairs.

Disclosures

No conflicts of interest, financial or otherwise, are declared by the author(s).

Acknowledgments

We thank Robert Bongard for help with the experiments.

Glossary

ACE
: Angiotensin-converting enzyme

BSA
: Bovine serum albumin

CoQ_9H_2
: Endogenous coenzyme Q_9 hydroquinone

DQH_2
: Durohydroquinone

$[DQ](x,t)$ and $[DQH_2](x,t)$
: Vascular concentrations of free DQ and DQH_2, respectively, at distance x from the capillary inlet and time t (μM)

[DQ]
: Total (free + BSA bound) vascular concentration of DQ (μM)

[DQH_2]
: Total (free + BSA bound) vascular concentration of DQH_2 (μM)

$h_c(t)$
: Capillary transit time distribution

FAPGG
: *N*-[3-(2-furyl) acryloyl]-Phe-Gly-Gly

K_{m1a}
: Apparent Michaelis-Menten constant for NQO1-mediated DQ reduction (μM)

K_{m2a}
: Apparent Michaelis-Menten constant for DQH_2 oxidation via complex III (μM)

k_{ox}
: Tissue-mediated DQH_2 oxidation rate on passage through the pulmonary circulation in the absence of rotenone (ml/min)

NQO1
: NAD(P)H:quinone oxidoreductase 1

PS
: Permeability-surface area product (ml/min), which is a measure of rate of ACE-mediated FAPGG hydrolysis, and an index of perfused capillary surface area

V_c
: Volume of the vascular region of the single capillary element model (ml)

V_e
: Volume of the tissue region of the single capillary element model (ml)

V_{max1}
: Maximum rate for DQ reduction via NQO1 (μmol/min)

V_{max2}
: Maximum rate for DQH_2 oxidation via complex III (μmol/min)

V_{F1}/α_1
: Virtual volume of distribution for DQ (ml)

V_{F2}/α_2
: Virtual volume of distribution for DQH_2 (ml)

W
: Convective transport velocity (cm/min)

Journal of Applied Physiology, Vol 111, No. 1 (July 2011): pg. 95-107. DOI.

Greek Letters

α_1 and α_2
: Constants that account for the rapidly equilibrating interactions of DQ and DQH_2 with the 5% BSA (i.e., P_c) perfusate

α_3 and α_4
: Constants that account for the rapidly equilibrating interactions of DQ and DQH_2 with lung tissue sites of association, respectively

Appendix

Based on the single capillary element model depicted in Fig. 6, the species balance equations descriptive of spatial and temporal variations in the concentrations of DQ, DQH_2 in (V_c and V_e) are

$$\frac{\partial[\overline{\mathrm{DQ}}]}{\partial t} + W\left(\frac{\mathrm{V}_c}{\mathrm{V}_c + \frac{\mathrm{V_{F1}}}{\alpha_1}}\right)\frac{\partial[\overline{\mathrm{DQ}}]}{\partial x} = \left(\frac{1}{\mathrm{V}_c + \frac{\mathrm{V_{F1}}}{\alpha_1}}\right)\left(\frac{V_{\mathrm{max2}}[\overline{\mathrm{DQH_2}}]}{K_{\mathrm{m2a}} + [\overline{\mathrm{DQH_2}}]} - \frac{V_{\mathrm{max1}}[\overline{\mathrm{DQ}}]}{K_{\mathrm{m1a}} + [\overline{\mathrm{DQ}}]}\right) \quad \text{(A1)}$$

$$\frac{\partial[\overline{\mathrm{DQH_2}}]}{\partial t} + W\left(\frac{\mathrm{V}_c}{\mathrm{V}_c + \frac{\mathrm{V_{F2}}}{\alpha_2}}\right)\frac{\partial[\overline{\mathrm{DQH_2}}]}{\partial x} = \left(\frac{1}{\mathrm{V}_c + \frac{\mathrm{V_{F2}}}{\alpha_2}}\right)\left(\frac{V_{\mathrm{max1}}[\overline{\mathrm{DQ}}]}{K_{\mathrm{m1a}} + [\overline{\mathrm{DQ}}]} - \frac{V_{\mathrm{max2}}[\overline{\mathrm{DQH_2}}]}{K_{\mathrm{m2a}} + [\overline{\mathrm{DQH_2}}]}\right) \quad \text{(A2)}$$

where W = convective transport velocity = $L/\bar{t}_c$; $x = 0$ and $x = L$ are the capillary inlet and outlet, respectively; $\bar{t}_c$ is the capillary mean transit time; $[DQ](x,t)$, and $[DQH_2](x,t)$ are vascular concentrations of free DQ and DQH_2 forms, respectively, at distance x from the capillary inlet and time t; $[DQ] = \alpha_1 [DQ]$ and $[DQH_2] = \alpha_2 [DQH_2]$ are the total

Journal of Applied Physiology, Vol 111, No. 1 (July 2011): pg. 95-107. DOI.

(free + BSA bound) vascular concentrations of DQ and DQH_2, respectively; $\alpha_1 = 1 +$ (DQ bound fraction/DQ free fraction) = 25 and $\alpha_2 = 1 +$ (DQH_2 bound fraction/DQH_2 free fraction) = 4.2 are constants that account for the rapidly equilibrating interactions of DQ and DQH_2, with the 5% BSA (i.e., P_c) perfusate calculated from the fractions of DQ and DQH_2 bound to BSA obtained by ultrafiltration (5). V_{max1} (μmol/min) and V_{max2} (μmol/min) are the respective maximum rates for DQ reduction via NQO1 and DQH_2 oxidation via complex III; K_{m1a} (μM) and K_{m2a} (μM) are the apparent Michaelis-Menten constants for NQO1 and complex III, respectively. $V_{F1}/\alpha_1 = (\alpha_3/\alpha_1)\, V_e$ and $V_{F2}/\alpha_2 = (\alpha_4/\alpha_2)\, V_e$ (ml) are the respective virtual volumes of distribution for DQ and DQH_2, where α_3 and α_4 are constants that account for the rapidly equilibrating interactions of DQ and DQH_2 with lung tissue sites (P_e) of association, respectively.

In the absence of rotenone, DQH_2 competes with CoQ_9H_2 for oxidation via complex III. This competition explains the observation that the rates of DQ efflux during DQH_2 infusion in the presence of dicumarol alone are lower than those in the presence of dicumarol plus rotenone (Figs. 3 and and5).5). Moreover, the steady-state DQ efflux rates during DQH_2 infusion in the presence of dicumarol alone appear to follow linear kinetics for the range of infused DQH_2 concentrations studied (Fig. 3). Thus, in the absence of rotenone, V_{max2} and K_{m2a} in *Eqs. A1* and *A2* are substituted for with a tissue-mediated DQH_2 oxidation rate k_{ox} (ml/min). *Equations A1* and *A2* become

$$\frac{\partial[\overline{\mathrm{DQ}}]}{\partial t} + W\left(\frac{\mathrm{V_c}}{\mathrm{V_c} + \frac{\mathrm{V_{F1}}}{\alpha_1}}\right)\frac{\partial[\overline{\mathrm{DQ}}]}{\partial x} = \left(\frac{1}{\mathrm{V_c} + \frac{\mathrm{V_{F1}}}{\alpha_1}}\right)\left(k_{\mathrm{ox}}[\overline{\mathrm{DQH_2}}] - \frac{V_{\mathrm{max1}}[\overline{\mathrm{DQ}}]}{K_{\mathrm{m1a}} + [\overline{\mathrm{DQ}}]}\right) \quad \text{(A3)}$$

Journal of Applied Physiology, Vol 111, No. 1 (July 2011): pg. 95-107. DOI.

$$\partial[\overline{\mathrm{DQH_2}}]\partial t + W\left(\frac{\mathrm{V_c}}{\mathrm{V_c} + \mathrm{V_{F2}}\alpha_2}\right)\frac{\partial[\overline{\mathrm{DQH_2}}]}{\partial x} = \left(\frac{1}{\mathrm{V_c} + \frac{\mathrm{V_{F2}}}{\alpha_2}}\right)\left(\frac{V_{\mathrm{max1}}[\overline{\mathrm{DQ}}]}{K_{\mathrm{m1a}} + [\overline{\mathrm{DQ}}]} - k_{\mathrm{ox}}[\overline{\mathrm{DQH_2}}]\right) \quad \text{(A4)}$$

Since our venous effluent data are measured at steady state, we considered the steady-state version of *Eqs. A1* and *A2* and *Eqs. A3* and *A4* obtained by setting all time derivative terms to zero. Thus *Eqs. A1* and *A2* and *Eqs. A3* and *A4* become *Eqs. A5* and *A6* and *Eqs. A7* and *A8*, respectively. Under steady-state conditions, the unknown model parameters are V_{max1}, V_{max2}, K_{m1a}, K_{m2a}, and k_{ox}.

$$W\mathrm{V}_c\frac{\partial[\overline{\mathrm{DQ}}]}{\partial x} = \left(\frac{V_{\mathrm{max2}}[\overline{\mathrm{DQH_2}}]}{K_{\mathrm{m2a}} + [\overline{\mathrm{DQH_2}}]} - \frac{V_{\mathrm{max1}}[\overline{\mathrm{DQ}}]}{K_{\mathrm{m1a}} + [\overline{\mathrm{DQ}}]}\right) \quad \text{(A5)}$$

$$W\mathrm{V}_c\frac{\partial[\overline{\mathrm{DQH_2}}]}{\partial x} = \left(\frac{V_{\mathrm{max1}}[\overline{\mathrm{DQ}}]}{K_{\mathrm{m1a}} + [\overline{\mathrm{DQ}}]} - \frac{V_{\mathrm{max2}}[\overline{\mathrm{DQH_2}}]}{K_{\mathrm{m2a}} + [\overline{\mathrm{DQH_2}}]}\right) \quad \text{(A6)}$$

$$W\mathrm{V}_c\frac{\partial[\overline{\mathrm{DQ}}]}{\partial x} = k_{\mathrm{ox}}[\overline{\mathrm{DQH_2}}] - \frac{V_{\mathrm{max1}}[\overline{\mathrm{DQ}}]}{K_{\mathrm{m1a}} + [\overline{\mathrm{DQ}}]} \quad \text{(A7)}$$

$$W\mathrm{V}_c\frac{\partial[\overline{\mathrm{DQH_2}}]}{\partial x} = \frac{V_{\mathrm{max1}}[\overline{\mathrm{DQ}}]}{K_{\mathrm{m1a}} + [\overline{\mathrm{DQ}}]} - k_{\mathrm{ox}}[\overline{\mathrm{DQH_2}}] \quad \text{(A8)}$$

Equations A1 and *A2* or *Eqs. A3* and *A4* are for a single capillary element. For the lung model, we accounted for the effect of the $h_c(t)$ on the plasma concentrations and redox status of DQ and DQH_2 on passage through the pulmonary circulation (5, 6). Previously, our laboratory determined $h_c(t)$ for normoxic rat lungs and hyper-85 lungs

and demonstrated that rat exposure to hyper-85 for 7 days decreased capillary mean transit time by 42% and increased the relative dispersion of $h_c(t)$ by 40% (52). These values were used in the kinetic analysis of the normoxic and hyper-85 lung data. For hyper-60 lungs, $h_c(t)$ was assumed to be the same as that determined for normoxic lungs. This is based on results in Table 1 that show exposure to hyper-60 for 7 days had no effect on perfused capillary surface area (*PS*) and on previous results that showed rat exposure to hyper-60 for 7 days had no significant effect on morphometrically measured lung capillary endothelial surface area and capillary volume (40).

Previously, our laboratory demonstrated that most of the dispersion within the lung vascular region is due to the capillary bed (52). Thus DQ and DQH_2 transit through the arteries and veins was represented by a shifted impulse function, where the shift is the plasma mean transit time through the arteries and veins, determined as previously described (52).

To model DQ or DQH_2 pulse infusions, given $h_c(t)$, *Eqs. A1* and *A2* or *Eqs. A3* and *A4* are solved numerically with appropriate initial ($t = 0$) and boundary ($x = 0$) conditions (5, 7, 8). To provide the whole organ output [DQ] and [DQH_2], the outputs for all transit times are summed, each weighted according to $h_c(t)$, as previously described (5, 7, 8).

References

[1] Ahmad S, White CW, Chang LY, Schneider BK, Allen CB. Glutamine protects mitochondrial structure and function in oxygen toxicity. Am J Physiol Lung Cell Mol Physiol 280: L779–L791, 2001

[2] Allen CB, Guo XL, White CW. Changes in pulmonary expression of hexokinase and glucose transporter mRNAs in rats adapted to hyperoxia. Am J Physiol Lung Cell Mol Physiol 274: L320–L329, 1998

[3] Allen CB, White CW. Glucose modulates cell death due to normobaric hyperoxia by maintaining cellular ATP. Am J Physiol Lung Cell Mol Physiol 274: L159–L164, 1998

[4] Altemeier WA, Sinclair SE. Hyperoxia in the intensive care unit: why more is not always better. Curr Opin Crit Care 13: 73–78, 2007

[5] Audi SH, Bongard RD, Dawson CA, Siegel D, Roerig DL, Merker MP. Duroquinone reduction during passage through the pulmonary

circulation. Am J Physiol Lung Cell Mol Physiol 285: L1116–L1131, 2003

[6] Audi SH, Bongard RD, Krenz GS, Rickaby DA, Haworth ST, Eisenhauer J, Roerig DL, Merker MP. Effect of chronic hyperoxic exposure on duroquinone reduction in adult rat lungs. Am J Physiol Lung Cell Mol Physiol 289: L788–L797, 2005

[7] Audi SH, Dawson CA, Ahlf SB, Roerig DL. Oxygen dependency of monoamine oxidase activity in the intact lung. Am J Physiol Lung Cell Mol Physiol 281: L969–L981, 2001

[8] Audi SH, Linehan JH, Krenz GS, Dawson CA. Accounting for the heterogeneity of capillary transit times in modeling multiple indicator dilution data. Ann Biomed Eng 26: 914–930, 1998

[9] Audi SH, Merker MP, Krenz GS, Ahuja T, Roerig DL, Bongard RD. Coenzyme Q1 redox metabolism during passage through the rat pulmonary circulation and the effect of hyperoxia. J Appl Physiol 105: 1114–1126, 2008

[10] Bassingthwaighte JB, Goresky CA, Linehan JH. Whole Organ Approaches to Cellular Metabolism: Permeation, Cellular Uptake, and Product Formation. New York: Springer, 1998

[11] Beattie DS, Japa S, Howton M, Zhu QS. Direct interaction between the internal NADH:ubiquinone oxidoreductase and ubiquinol:cytochrome c oxidoreductase in the reduction of exogenous quinones by yeast mitochondria. Arch Biochem Biophys 292: 499–505, 1992

[12] Beyer RE, Segura-Aguilar J, Di Bernardo S, Cavazzoni M, Fato R, Fiorentini D, Galli MC, Setti M, Landi L, Lenaz G. The role of DT-diaphorase in the maintenance of the reduced antioxidant form of coenzyme Q in membrane systems. Proc Natl Acad Sci U S A 93: 2528–2532, 1996

[13] Bongard RD, Lindemer BJ, Krenz GS, Merker MP. Preferential utilization of NADPH as the endogenous electron donor for NAD(P)H:quinone oxidoreductase 1 (NQO1) in intact pulmonary arterial endothelial cells. Free Radic Biol Med 46: 25–32, 2009

[14] Boveris A, Oshino R, Erecinska M, Chance B. Reduction of mitochondrial components by durohydroquinone. Biochim Biophys Acta 245: 1–16, 1971

[15] Brueckl C, Kaestle S, Kerem A, Habazettl H, Krombach F, Kuppe H, Kuebler WM. Hyperoxia-induced reactive oxygen species formation in pulmonary capillary endothelial cells in situ. Am J Respir Cell Mol Biol 34: 453–463, 2006

[16] Cadenas E. Antioxidant and prooxidant functions of DT-diaphorase in quinone metabolism. Biochem Pharmacol 49: 127–140, 1995

[17] Cadenas E, Boveris A, Ragan CI, Stoppani AO. Production of superoxide radicals and hydrogen peroxide by NADH-ubiquinone reductase and

ubiquinol-cytochrome c reductase from beef-heart mitochondria. Arch Biochem Biophys 180: 248–257, 1977

[18] Campian JL, Qian M, Gao X, Eaton JW. Oxygen tolerance and coupling of mitochondrial electron transport. J Biol Chem 279: 46580–46587, 2004

[19] Capellier G, Maupoil V, Boussat S, Laurent E, Neidhardt A. Oxygen toxicity and tolerance. Minerva Anestesiol 65: 388–392, 1999

[20] Cho HY, Jedlicka AE, Reddy SP, Kensler TW, Yamamoto M, Zhang LY, Kleeberger SR. Role of NRF2 in protection against hyperoxic lung injury in mice. Am J Respir Cell Mol Biol 26: 175–182, 2002

[21] Chow CW, Herrera Abreu MT, Suzuki T, Downey GP. Oxidative stress and acute lung injury. Am J Respir Cell Mol Biol 29: 427–431, 2003

[22] Clark JM, Lambertsen CJ. Pulmonary oxygen toxicity: a review. Pharmacol Rev 23: 37–133, 1971

[23] Coursin DB, Cihla HP, Will JA, McCreary JL. Adaptation to chronic hyperoxia. Biochemical effects and the response to subsequent lethal hyperoxia. Am Rev Respir Dis 135: 1002–1006, 1987

[24] Crapo JD, Barry BE, Foscue HA, Shelburne J. Structural and biochemical changes in rat lungs occurring during exposures to lethal and adaptive doses of oxygen. Am Rev Respir Dis 122: 123–143, 1980

[25] Crapo JD, Peters-Golden M, Marsh-Salin J, Shelburne JS. Pathologic changes in the lungs of oxygen-adapted rats: a morphometric analysis. Lab Invest 39: 640–653, 1978

[26] Crapo JD, Tierney DF. Superoxide dismutase and pulmonary oxygen toxicity. Am J Physiol 226: 1401–1407, 1974

[27] Davis WB, Rennard SI, Bitterman PB, Crystal RG. Pulmonary oxygen toxicity. Early reversible changes in human alveolar structures induced by hyperoxia. N Engl J Med 309: 878–883, 1983

[28] Desquiret V, Gueguen N, Malthiery Y, Ritz P, Simard G. Mitochondrial effects of dexamethasone imply both membrane and cytosolic-initiated pathways in HepG2 cells. Int J Biochem Cell Biol 40: 1629–1641, 2008

[29] Dinkova-Kostova AT, Talalay P. Persuasive evidence that quinone reductase type 1 (DT diaphorase) protects cells against the toxicity of electrophiles and reactive forms of oxygen. Free Radic Biol Med 29: 231–240, 2000

[30] Fisher AB, Beers MF. Hyperoxia and acute lung injury. Am J Physiol Lung Cell Mol Physiol 295: L1066–L1067, 2008

[31] Fisher AB, Forman HJ, Glass M. Mechanisms of pulmonary oxygen toxicity. Lung 162: 255–259, 1984

[32] Frank L, Bucher JR, Roberts RJ. Oxygen toxicity in neonatal and adult animals of various species. J Appl Physiol 45: 699–704, 1978

[33] Frank L, Iqbal J, Hass M, Massaro D. New "rest period" protocol for inducing tolerance to high O2 exposure in adult rats. Am J Physiol Lung Cell Mol Physiol 257: L226–L231, 1989

[34] Freeman BA, Crapo JD. Hyperoxia increases oxygen radical production in rat lungs and lung mitochondria. J Biol Chem 256: 10986–10992, 1981

[36] Gao L, Barnes KC. Recent advances in genetic predisposition to clinical acute lung injury. Am J Physiol Lung Cell Mol Physiol 296: L713–L725, 2009

[37] Gonzalez-Aragon D, Ariza J, Villalba JM. Dicoumarol impairs mitochondrial electron transport and pyrimidine biosynthesis in human myeloid leukemia HL-60 cells. Biochem Pharmacol 73: 427–439, 2007

[38] Griffith DE, Holden WE, Morris JF, Min LK, Krishnamurthy GT. Effects of common therapeutic concentrations of oxygen on lung clearance of 99mTc DTPA and bronchoalveolar lavage albumin concentration. Am Rev Respir Dis 134: 233–237, 1986

[39] Griffith OW. Determination of glutathione and glutathione disulfide using glutathione reductase and 2-vinylpyridine. Anal Biochem 106: 207–212, 1980

[40] Hayatdavoudi G, O'Neil JJ, Barry BE, Freeman BA, Crapo JD. Pulmonary injury in rats following continuous exposure to 60% O_2 for 7 days. J Appl Physiol 51: 1220–1231, 1981

[41] Ho YS. Transgenic and knockout models for studying the role of lung antioxidant enzymes in defense against hyperoxia. Am J Respir Crit Care Med 166: S51–S56, 2002

[42] Ho YS, Dey MS, Crapo JD. Antioxidant enzyme expression in rat lungs during hyperoxia. Am J Physiol Lung Cell Mol Physiol 270: L810–L818, 1996

[43] Kimball RE, Reddy K, Peirce TH, Schwartz LW, Mustafa MG, Cross CE. Oxygen toxicity: augmentation of antioxidant defense mechanisms in rat lung. Am J Physiol 230: 1425–1431, 1976

[44] Lenaz G, Fato R, Baracca A, Genova ML. Mitochondrial quinone reductases: complex I. Methods Enzymol 382: 3–20, 2004

[45] Li J, Gao X, Qian M, Eaton JW. Mitochondrial metabolism underlies hyperoxic cell damage. Free Radic Biol Med 36: 1460–1470, 2004

[46] Mantell LL, Horowitz S, Davis JM, Kazzaz JA. Hyperoxia-induced cell death in the lung–the correlation of apoptosis, necrosis, and inflammation. Ann N Y Acad Sci 887: 171–180, 1999

[47] O'Brodovich HM, Mellins RB. Bronchopulmonary dysplasia. Unresolved neonatal acute lung injury. Am Rev Respir Dis 132: 694–709, 1985

[48] Otterbein LE, Choi AM. The saga of leucine zippers continues: in response to oxidative stress. Am J Respir Cell Mol Biol 26: 161–163, 2002

[49] Owens CW, Belcher RV. A colorimetric micro-method for the determination of glutathione. Biochem J 94: 705–711, 1965

[50] Phua J, Badia JR, Adhikari NK, Friedrich JO, Fowler RA, Singh JM, Scales DC, Stather DR, Li A, Jones A, Gattas DJ, Hallett D, Tomlinson G, Stewart TE, Ferguson ND. Has mortality from acute respiratory distress syndrome decreased over time?: A systematic review. Am J Respir Crit Care Med 179: 220–227, 2009

[51] Radjendirane V, Joseph P, Lee YH, Kimura S, Klein-Szanto AJ, Gonzalez FJ, Jaiswal AK. Disruption of the DT diaphorase (NQO1) gene in mice leads to increased menadione toxicity. J Biol Chem 273: 7382–7389, 1998

[52] Ramakrishna M, Gan Z, Clough AV, Molthen RC, Roerig DL, Audi SH. Distribution of capillary transit times in isolated lungs of oxygen-tolerant rats. Ann Biomed Eng 38: 3449–3465, 2010

[53] Ratner V, Starkov A, Matsiukevich D, Polin RA, Ten VS. Mitochondrial dysfunction contributes to alveolar developmental arrest in hyperoxia-exposed mice. Am J Respir Cell Mol Biol 40: 511–518, 2009

[54] Rogers LK, Tipple TE, Nelin LD, Welty SE. Differential responses in the lungs of newborn mouse pups exposed to 85% or >95% oxygen. Pediatr Res 65: 33–38, 2009

[55] Ross D, Kepa JK, Winski SL, Beall HD, Anwar A, Siegel D. NAD(P)H:quinone oxidoreductase 1 (NQO1): chemoprotection, bioactivation, gene regulation and genetic polymorphisms. Chem Biol Interact 129: 77–97, 2000

[56] Ross D, Siegel D, Beall H, Prakash AS, Mulcahy RT, Gibson NW. DT-diaphorase in activation and detoxification of quinones. Bioreductive activation of mitomycin C. Cancer Metastasis Rev 12: 83–101, 1993

[57] Saugstad OD. Optimal oxygenation at birth and in the neonatal period. Neonatology 91: 319–322, 2007

[58] Schoonen WG, Wanamarta AH, van der Klei-van Moorsel JM, Jakobs C, Joenje H. Respiratory failure and stimulation of glycolysis in Chinese hamster ovary cells exposed to normobaric hyperoxia. J Biol Chem 265: 1118–1124, 1990

[59] Siegel D, Gustafson DL, Dehn DL, Han JY, Boonchoong P, Berliner LJ, Ross D. NAD(P)H:quinone oxidoreductase 1: role as a superoxide scavenger. Mol Pharmacol 65: 1238–1247, 2004

[60] Siegel D, Ross D. Immunodetection of NAD(P)H:quinone oxidoreductase 1 (NQO1) in human tissues. Free Radic Biol Med 29: 246–253, 2000

[61] Storrie B, Madden EA. Isolation of subcellular organelles. Methods Enzymol 182: 203–225, 1990

[62] Suttorp N, Toepfer W, Roka L. Antioxidant defense mechanisms of endothelial cells: glutathione redox cycle versus catalase. Am J Physiol Cell Physiol 251: C671–C680, 1986

[63] Tan AS, Berridge MV. Evidence for NAD(P)H:quinone oxidoreductase 1 (NQO1)-mediated quinone-dependent redox cycling via plasma membrane electron transport: a sensitive cellular assay for NQO1. Free Radic Biol Med 48: 421–429, 2010

[64] Tierney D, Ayers L, Herzog S, Yang J. Pentose pathway and production of reduced nicotinamide adenine dinucleotide phosphate. A mechanism that may protect lungs from oxidants. Am Rev Respir Dis 108: 1348–1351, 1973

[65] Tietze F. Enzymic method for quantitative determination of nanogram amounts of total and oxidized glutathione: applications to mammalian blood and other tissues. Anal Biochem 27: 502–522, 1969

[66] Turrens JF. Mitochondrial formation of reactive oxygen species. J Physiol 552: 335–344, 2003

[67] Van Klaveren RJ, Dinsdale D, Pype JL, Demedts M, Nemery B. Changes in gamma-glutamyltransferase activity in rat lung tissue, BAL, and type II cells after hyperoxia. Am J Physiol Lung Cell Mol Physiol 273: L537–L547, 1997

[68] Von Jagow G, Bohrer C. Inhibition of electron transfer from ferrocytochrome b to ubiquinone, cytochrome c1 and duroquinone by antimycin. Biochim Biophys Acta 387: 409–424, 1975

[69] Wang Y, Feinstein SI, Manevich Y, Ho YS, Fisher AB. Lung injury and mortality with hyperoxia are increased in peroxiredoxin 6 gene-targeted mice. Free Radic Biol Med 37: 1736–1743, 2004

[70] Whitney PL, Frank L. Does lung NAD(P)H:quinone reductase (DT-diaphorase) play an antioxidant enzyme role in protection from hyperoxia? Biochim Biophys Acta 1156: 275–282, 1993

[71] Zhu H, Jia Z, Mahaney JE, Ross D, Misra HP, Trush MA, Li Y. The highly expressed and inducible endogenous NAD(P)H:quinone oxidoreductase 1 in cardiovascular cells acts as a potential superoxide scavenger. Cardiovasc Toxicol 7: 202–211, 2007

[72] Zhu QS, Beattie DS. Direct interaction between yeast NADH-ubiquinone oxidoreductase, succinate-ubiquinone oxidoreductase, and ubiquinol-cytochrome c oxidoreductase in the reduction of exogenous quinones. J Biol Chem 263: 193–199, 1988

Corresponding author.
Address for reprint requests and other correspondence: S. H. Audi, Research Service 151, Zablocki VAMC, 5000 W. National Ave., Milwaukee, WI 53295 (e-mail: said.audi@mu.edu